

## Noise Emission in Large Aspect Ratio Cavities

G. Guj<sup>1</sup>, R. Camussi<sup>1</sup>, A. Di Marco<sup>1</sup> and A. Ragni<sup>2</sup>

<sup>1</sup>Industrial and Mechanical Engineering Department (DIMI)  
 Roma Tre University, Rome, 00146 ITALY

<sup>2</sup>Department of Experimental Aerodynamics Methodologies  
 Italian Aerospace Research Centre (CIRA), Capua, 81043 ITALY

### Abstract

This paper describes an experimental test campaign aimed at the study of the influence of surface irregularities on the turbulent boundary layer noise emission. The irregularities were represented by a two-steps large aspect-ratio cavity. The main task of the experiments was to characterize, from the aeroacoustic and fluid-dynamic viewpoint, the effects of the main non-dimensional parameters on the statistical quantities of interest correlated to the wall pressure fluctuations, accounting for the geometrical and dynamical similarity requirements with respect to real conditions. The experiments were performed in the low speed wind tunnel at ENEA-DIMI research centre. Results allowed us to individuate the significant, independent dimensionless groups governing the point wall pressure spectra in-between the double steps discontinuity. Proper scaling relations of local (pressure spectra) and global (Sound Pressure Level - *SPL*) quantities are proposed, and universal form functions modelling the properly normalized spectra and *SPL* are presented. The ability of the proposed model to predict the noise emission is finally validated and tested on experimental data.

### List of Symbols

$\alpha_i$	Power laws coefficients
$B$	Cavity span
$c$	Speed of sound
$\delta$	Boundary layer thickness
$f$	Frequency
$G_{pp}$	Pressure auto-spectrum
$H$	Steps height
$L$	Cavity length
$q$	Dynamic pressure
$Re$	Reynolds number
$St$	Strouhal Number
$U$	Free stream velocity
$x$	Streamwise coordinate
$\Delta$	Thickness ratio
$\Gamma_{pp}$	Universal spectrum
$\Psi$	Universal form function
$\gamma$	Velocity ratio
$\nu$	Cinematic viscosity
$\tilde{u}$	Mean Turbul. level within TBL
$\sigma$	Standard deviation
$\langle \quad \rangle$	Dimensionless quantity
$AR$	Aspect ratio
$\langle \quad \rangle$	Average on the tests
$\overline{\quad}$	Average on $x$ position

### Introduction

Steps and geometrical irregularities on the exterior surface of modern high-speed passengers aircraft appear for example at skin lap joints or window gaskets, and are recognized as potential sources of aerodynamically generated noise. It is known that the contributions of such aeroacoustic sources to the interior noise is significant and dominate the overall interior noise at the front part of the fuselage. Similar aeroacoustic problems are also encountered in other fields of engineering interest, for example in the vehicles or trains aerodynamics. Even if the subject is of great interest from the viewpoint of practical and basic research applications, it has not been treated in detail and the results available in literature are limited and sometimes contradictory.

The primary motivation of the present work is to cover the lack of experimental results in this field and the main goal is to contribute to a deeper understanding of the physics through a detailed experimental analysis. The surface irregularities were modelled by a backward-facing step (BFS) followed by a forward-facing step (FFS) disposed in an incompressible turbulent boundary layer (TBL). The sketch of the surface irregularities model is exhibited in Fig. 1, together with the main symbols used in present work.

When the flow reaches the BFS, a detachment occurs and a reverse flow zone is generated just after the step. After a distance of about  $5-7H$  there is an oscillating reattachment point of the flow. The reattachment point unsteadiness is recognised a strong noise source [1], [2]. After the reattachment, the flow encounters the FFS and the flow behaviour can be described as follow [3], [4]: there is a flow detachment about  $1H$  before the step, a separation bubble close to the step in which reverse flow occurs, and a second recirculating region bounded downstream by a reattachment point, after which the TBL slowly recovers its characteristics.

### Dimensional Analysis and Scalings

The six significative dimensionless groups governing the point wall pressure spectra in-between the double steps discontinuity are:

$$G'_{pp} = \frac{G_{pp} U}{q^2 H}, \quad St_H = \frac{fH}{U}, \quad Re_H = \frac{UH}{\nu}, \quad \gamma = \frac{\tilde{u}}{U},$$

$$x' = \frac{x}{H}, \quad \Delta = \frac{\delta}{H} \quad (1)$$

with

$$\tilde{u} = \frac{1}{\delta} \int_0^{\delta} \sigma_u dy \quad (2)$$

The effect of the other non-significative groups, (L/H,  $U_\infty/c$  and B/H) is neglected.

The study was conducted by means of the hypothesis of the variables separation. Thus the single dimensionless spectrum  $G'_{pp}$  can be represented as a function of the dimensionless groups, leading to the following expressions:

$$\begin{aligned} G'_{pp}(St_H, x', \Delta, Re_H, \gamma) &= G''_{pp}(St_H, x') \Delta^{\alpha_1} Re_H^{\alpha_2} \gamma^{\alpha_3} \\ &= G'''_{pp}(St_H) \Psi(x') \Delta^{\alpha_1} Re_H^{\alpha_2} \gamma^{\alpha_3} \end{aligned} \quad (3)$$

The quantity  $G'''_{pp}(St_H)$  denotes spectra with corresponding unitary  $SPL'''$ . Therefore, the basic hypothesis, which is here made, is the assumption of a universal shape of the spectra  $G'''_{pp}(St_H)$ . The actual amplitude modulation due to the effect of the distance from the steps, is recovered by the function  $\Psi(x')$  which denotes a universal form function representing the normalized  $SPL$  variation along the dimensionless axial variable  $x'$ . So, the problem is if it is possible to determinate the  $\alpha_i$  coefficients and the universal function  $\Psi(x')$  so that the dimensionless spectra  $G'''_{pp}$  collapse on a reasonable unique shape with unitary  $SPL'''$ . Then, a unique spectrum form function  $\Gamma_{pp}$  can be obtained by an average procedure on a very large number of  $G'''_{pp}$ . Details about the data analysis are reported in the following sections. In order to better understand the adopted procedure is useful to define the following quantities:

$$SPL' = 10 \log_{10} \left[ \int_0^{St_{H \max}} G'_{pp} dSt_H \right] \quad (4)$$

$$SPL'' = 10 \log_{10} \left[ \int_0^{St_{H \max}} G''_{pp} dSt_H \right] \quad (5)$$

Integrating the eqn (3), taking the logarithm and using the expression (4), the following relation is obtained:

$$SPL' = \alpha_1 10 \log_{10} \Delta + \alpha_2 10 \log_{10} Re + \alpha_3 10 \log_{10} \gamma + SPL'' \quad (6)$$

The unitary  $SPL'''$  is obtained as follows:

$$\begin{aligned} SPL''' &= \langle -10 \log_{10} \Psi(x') + SPL'' \rangle \\ &= \langle \tilde{\Psi}(x') + SPL'' \rangle = 1 \end{aligned} \quad (7)$$

The symbols  $\langle \rangle$  represent the average on the tests. The universal form function of the  $SPL$ ,  $\Psi(x')$ , is calculated from equ. (7).

### Experimental Apparatus

The tests were carried out in the low-speed wind tunnel installed at the aerodynamic laboratory of the Energy Department of ENEA.

The steps were obtained using aluminium plates of the same height  $H$ , which were mounted in different positions to obtain different cavity length  $L$ ; the cavity span  $B$  is much larger than  $H$  ( $B/H \gg 1$ ). Measurements inside the cavity were performed using an aluminium sliding plate as cavity floor. Four microphones can be positioned on the cavity and flush mounted on the floor, three streamwise and one spanwise. TBL of desired characteristics

were obtained with a special designed generator constituted by curved grids placed at the end of the convergent.

The pressure fluctuations measurements were performed using B&K equipment: 1/4'' 4135 & 1/8'' 4138 microphones, Falcon 2670 preamplifiers, Nexus 2690 for sensitivity, amplification and filters settings. The pressure signals were acquired using an 8 channel Yokogawa *Digital Scope* DL708E. Around  $10^5$  samples, with a sampling rate in the range 10kHz-40kHz and a cut-off frequency filter in the range 4kHz-20kHz, were acquired from each channel.

A preliminary TBL aerodynamic characterisation was performed using a hot wire anemometer. The sliding plate was translated by means of a numerically controlled micrometric traversing system driven by a step-by-step motor.

### Test Matrix

The measurements were performed at thirty different positions along the cavity floor (Fig. 1).

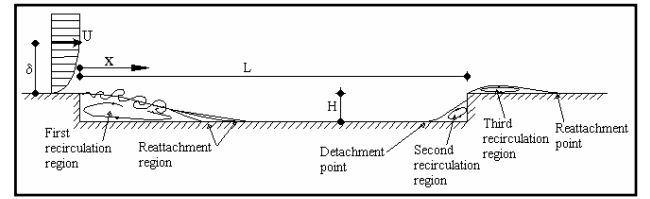


Fig. 1: Sketch of flow conditions over a backward-forward facing step.

The use of more microphones at the wall was useful to check the reliability of the results. Measurements were also performed in fixed positions downstream the FFS. During the whole test campaign a reference microphone was placed in the flow field to measure the background noise. The values assumed by the most important geometrical and aerodynamic parameters during the tests are reported in Tab. 1.

$U$ [m/s]	10, 30, 50
$H$ [mm]	15, 25
$\delta$ [mm]	22, 25, 28, 100, 150, 165
$L$ [mm]	340, 640
$Re_H$ [ $10^4$ ]	1, 1.7, 3.1, 5.1
$Re_\delta$ [ $10^4$ ]	1.9, 5.1, 7.5, 10.3, 20.5, 56.5

Tab.1: Values of the aerodynamic parameters assumed during the tests.

Such values were defined accounting for real conditions experienced by aircraft manufacturers. The low TBL thicknesses are relative to the natural TBL present on the test section floor, whereas the high thicknesses were generated using a curved grid.

### Data Post-processing Procedure

The adopted procedure to analyse the microphone signals is summarised below.

1. The pressure spectra  $G_{pp}$  are calculated, and corrected for the wind tunnel background noise. Details about the adopted conditioning technique can be found in [1].
2. The dimensionless spectra  $G'_{pp}$  (and  $SPL'$ ) are calculated from equ (1).
3. The exponents  $\alpha_1$ ,  $\alpha_2$ ,  $\alpha_3$ , are determined by applying an optimization procedure which minimizes the  $SPL'''$  deviations.
4. The functions  $G''_{pp}$  and  $SPL''$  are then definitively calculated using equ (3) and (6) and the optimum set of exponents  $\alpha_i$ .
5. Using equ (7) the  $\Psi$  function can be calculated at each  $x'$  position, averaging on a large number of tests (order of 400).

6. Once the universal form function  $\Psi$  is calculated, the functions  $G''_{pp}$ ,  $G'''_{pp}$  can be calculated using equations (3).
7. The universal form function  $\Gamma_{pp}$  representing the spectra is obtained as follows, where the over bar indicates the average on  $x'$  positions.

$$\Gamma_{pp} = \left\langle \overline{G''_{pp}}(St_H) \right\rangle \quad (8)$$

### Results

A comparison among normalized spectra  $G'_{pp}(St_H)$  measured at the reattachment point and those by other authors is reported in Fig. 2.

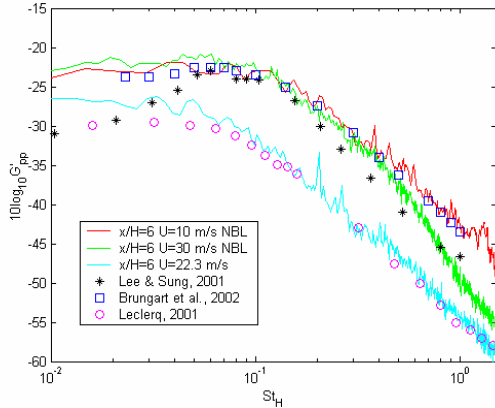


Fig. 2: Spectra comparison.

The reported reference measurements were obtained at the reattachment point downstream BFS, and the agreement with present data is satisfactory for both the natural (NBL) and the artificial boundary layer cases. It is also noticeable that the normalization adopted to obtain the  $G'_{pp}(St_H)$  is not sufficient to collapse the spectra, so the other parameters described in the previous sections have to be taken into account.

A typical spatio-frequency pressure spectrogram in the cavity (Fig. 3) shows that the energy content is concentrated at low frequencies while the spectra amplitude is modulated by the  $SPL$  distribution.

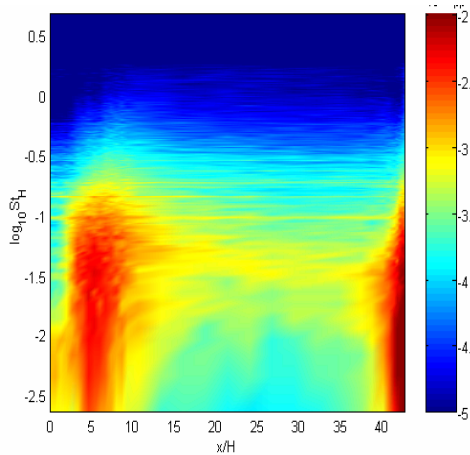


Fig. 3: Pressure spectrogram.

This result supports the idea presented in the previous sections where the scaling of the spectra is obtained by normalizing their amplitudes in terms of the function  $\Psi$ , which reproduces the  $SPL$  distribution along the cavity. The thin horizontal lines that can be observed in the picture represent some background noise not completely eliminated by the correction procedure.

The  $SPL$  distributions along the cavity model, for different flow conditions, are reported in Fig. 4.

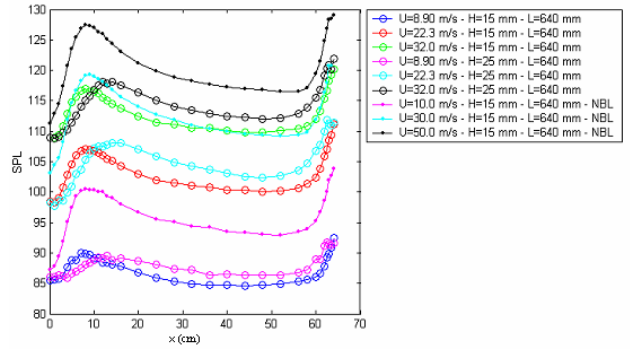


Fig. 4:  $SPL$  distributions along the cavity for different flow conditions.

In the different reported tests, steps' height, free stream velocity, steps' separation and incoming boundary layer thickness were varied and a clear influence on the  $SPL$  amplitude is observable. However, a similarity in shape of the  $SPL(x)$  is exhibited indicating that a collapse of the curves could be obtained by a proper rescaling. From the physical viewpoint, it is stressed that the first maximum of  $SPL$  occurs in the region of the average reattachment point of the separation bubble downstream the BFS (Fig. 1). The second maximum is located at the end of the step floor, just in front of the FFS; this maximum is probably due to the reattachment of the flow on the vertical face of the step. It is also shown that the second maximum is larger than the first one, thus indicating that the FFS configuration is more effective in emitting noise.

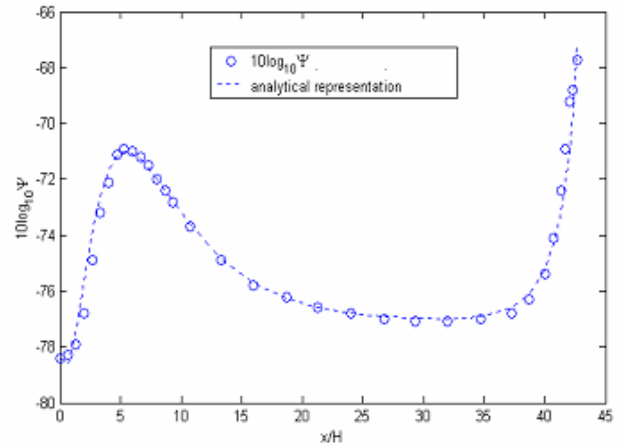


Fig. 5: Universal form function.

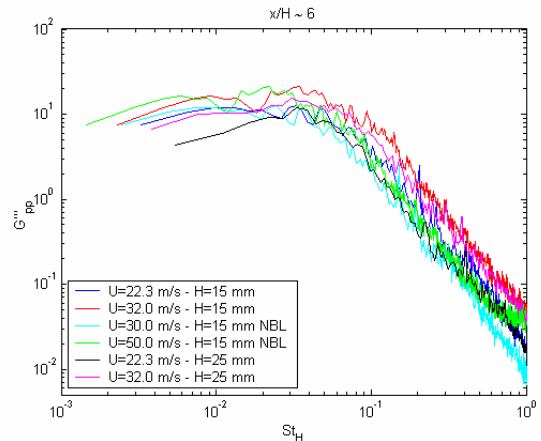


Fig. 6: Normalized spectra.

Applying the procedure described in the previous section the following exponents are obtained:  $\alpha_1 = -1.2$ ,  $\alpha_2 = -0.1$ ,  $\alpha_3 = -3.3$ .

The universal form function  $\Psi$  is exhibited in Fig. 5.

Using the calculated exponents  $\alpha_i$  and the universal function  $\Psi$ , the normalized spectra  $G''''_{pp}$  can be calculated at different  $x'$  positions (Fig. 6).

As it is possible to observe, the shape of the spectra is almost the same and a good collapsing is obtained.

As described in the previous section, averaging the normalised spectra  $G''''_{pp}$  on different test conditions and different  $x'$  positions, the universal form function can be extracted by a best fitting procedure, based on the minimization of the mean square error: all the considered spectra are included, except those ones used for the validation purposes (Fig. 7).

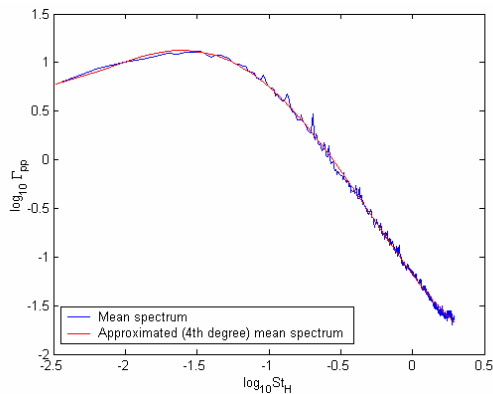


Fig. 7: Universal shape for the pressure spectrum.

The validation of the proposed model for the calculation of the noise  $SPL$  in a cavity is conducted using the model to simulate the considered cases, and comparing the simulated results with the measured and conditioned  $SPL$ . The mean difference between the simulated and measured  $SPL$ , evaluated from all the test cases and positions, is lower than  $1.4$  dB. An example of the comparison between simulated and measured spectra is reported in Fig. 8. The comparison is relative to a streamwise position where the agreement between measured and simulated quantities is good but (as already mentioned) this is not true very close to the vertical side of the BFS.

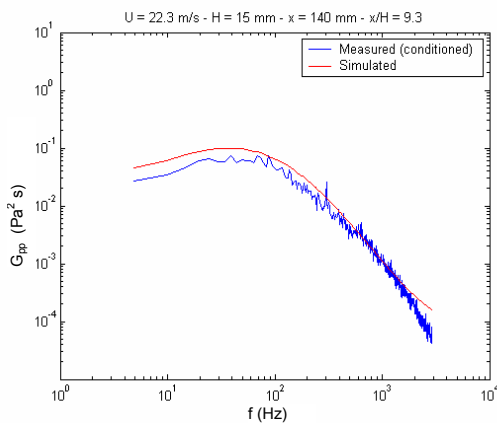


Fig. 8: Measured and simulated pressure spectrum

## Conclusions

In the present report, results aimed to the aeroacoustic characterization of TBL on a surface with geometrical irregularities have been presented. The experimental analysis was conducted on a two-step (backward/forward facing step) large aspect-ratio cavity and the main results obtained are summarized as follows.

- The dimensional analysis allowed individuating six relevant parameters influencing the aeroacoustic behaviour.
- From the physical viewpoint, the  $SPL$  distributions along the plate evidenced that the dimensionless reattachment point downstream the first BFS is weakly influenced by the dimensionless parameters and it is always located at  $5-6H$ . Furthermore it is observed that the maximum  $SPL$  is reached in the vicinity of the second step, thus confirming that the FFS is more effective in emitting noise. We argue that the largest noise emission at the second step are not attributed to localized fluid dynamic events, but rather to acoustic effects probably related to the reattachment of the flow at the vertical wall.
- The experimental results confirmed that the variables separation approach is appropriate. Indeed, both the wall pressure spectra and  $SPL$  distributions along the cavity show a satisfactory similarity in their shape, at least within the regions not too close to the two steps, where re-circulations occur. The spectra dependence upon the dimensionless parameters is determined by power laws (yielding to a linear dependence in terms of  $SPL$ ) and an optimisation procedure was applied to retrieve the best (in terms of minimum error) scaling exponents. Furthermore, it was found that the parameter  $L/H$ , being asymptotic, can be neglected, while the exponent of the  $Re_H$  number is very small and thus this number does play a weak role.

## References

- [1] Bendat, J.S., Piersol, A.G., *Random Data: Analysis and Measurements Procedures*, Wiley Interscience, 1986.
- [2] Efimtsov, B.M., Kozlov, N.M., Kravchenko, S.V., Anderson, A.O., Wall Pressure Fluctuation Spectra at Small Forward-Facing Step, *Proceedings of the 5<sup>th</sup> AIAA/CEAS Aeroacoustics Conference - AIAA paper 99-1964*, Bellevue, WA, USA, 1999.
- [3] Lauchle, G.C., Kargus, W.A., Scaling of Turbulent Wall Pressure Fluctuations Downstream of a Rearward-Facing Step, *J. Acoust. Soc. Am.*, **107**, 2001, L1-L6.
- [4] Leclercq, D.J.J., Jacob, M.C., Louisot, A., Talotte, C., Forward-backward Facing Step Pair: aerodynamic flow, wall pressure and acoustic characterisation, *Proceedings of the 7<sup>th</sup> AIAA/CEAS Aeroacoustics Conference - AIAA paper 2001-1249*, Maastricht, The Netherlands, 2001.
- [5] Lee, I., Sung, H.J., Characteristics of Wall Pressure Fluctuations in Separated and Reattaching Flows over a Backward-Facing Step – Part I, *Exp. Fluids*, **30**, 2001, 262-272.